Plant Science 348 (2024) 112231

Contents lists available at ScienceDirect

Plant Science

journal homepage: www.elsevier.com/locate/plantsci

Eight hydroxyproline-*O*-galactosyltransferases play essential roles in female reproductive development

Diana Moreira [a,1,2], Dasmeet Kaur [b,c,1], Sara Fourbert-Mendes [a], Allan M. Showalter [b,c], Sílvia Coimbra [a], Ana Marta Pereira [a,*]

[a] LAQV Requimte, Sustainable Chemistry, Departamento de Biologia, Faculdade de Ciências da Universidade do Porto, Porto 4169-007, Portugal
[b] Department of Environmental & Plant Biology, Ohio University, Athens, OH 45701-2979, USA
[c] Molecular and Cellular Biology Program, Ohio University, Athens, OH 45701-2979, USA

ARTICLE INFO

Keywords:
Arabinogalactan-Proteins
Female gametophyte development
Hyp-Galactosyltransferases
Plant reproduction
Pollen-pistil interactions

ABSTRACT

In angiosperms, ovules give rise to seeds upon fertilization. Thus, seed formation is dependent on both successful ovule development and tightly controlled communication between female and male gametophytes. During establishment of these interactions, cell walls play a pivotal role, especially arabinogalactan-proteins (AGPs). AGPs are highly glycosylated proteins decorated by arabinogalactan side chains, representing 90 % of the AGP molecule. AGP glycosylation is initiated by a reaction catalysed by hydroxyproline-*O*-galactosyltransferases (Hyp-GALTs), specifically eight of them (GALT2–9), which add the first galactose to Hyp residues. Five Hyp-GALTs (GALT2, 5, 7, 8 and 9) were previously described as essential for AGP functions in pollen and ovule development, pollen-pistil interactions, and seed morphology. In the present work, a higher order Hyp-GALT mutant (*23456789*) was studied, with a high degree of under-glycosylated AGPs, to gain deeper insight into the crucial roles of these eight enzymes in female reproductive tissues. Notably, the *23456789* mutant demonstrated a high quantity of unfertilized ovules, displaying abnormal callose accumulation both at the micropylar region and, sometimes, throughout the entire embryo sac. Additionally, this mutant displayed ovules with abnormal embryo sacs, had a disrupted spatiotemporal distribution of AGPs in female reproductive tissues, and showed abnormal seed and embryo development, concomitant with a reduction in AGP-GlcA levels. This study revealed that at least three more enzymes exhibit Hyp-*O*-GALT activity in Arabidopsis (GALT3, 4 and 6), and reinforces the crucial importance of AGP carbohydrates in carrying out the biological functions of AGPs during plant reproduction.

1. Introduction

In Arabidopsis, the ovule is formed by the female gametophyte (FG) - the embryo sac - and its surrounding sporophytic tissues. Ovule development includes two different processes: megasporogenesis and megagametogenesis (Drews et al., 1998; Drews and Yadegari, 2002; Qin et al., 2023; Schneitz et al., 1997, 1995). During megasporogenesis, the proximal - distal polarity is established, while during megagametogenesis, the mature FG is formed (Colombo et al., 2008; Reiser and Fischer, 1993). Thus, a mature ovule consists of the embryo sac enclosing three antipodal cells at the proximal region, one central cell, and one egg cell surrounded by two synergids at the distal region, surrounded by sporophytic cells - two integuments that leave an opening at its micropylar end (Schneitz et al., 1997, 1995; Yadegari, 2004) for pollen tube (PT) entrance. Following normal development of female and male gametophytes (pollen grain), flowering plants reproduce sexually through the unique process of double fertilization. This begins with the arrival of pollen grains (PG) at the stigma of the pistil leading to PT germination. The PT transports the two sperm cells through the female tissues until they reach the ovules. Near the ovule, PTs direct their growth towards the micropyle, entering the embryo sac. Subsequently, the two sperm cells are released and fuse with the female gametes - the

* Corresponding author.
E-mail address: ambacpereira@fc.up.pt (A.M. Pereira).
[1] Both authors contributed equally to this manuscript
[2] Present address: Universidade Católica Portuguesa, CBQF – Centro de Biotecnologia e Química Fina – Laboratório Associado, Escola Superior de Biotecnologia, Rua Diogo Botelho 1327, 4169–005, Porto, Portugal

https://doi.org/10.1016/j.plantsci.2024.112231
Received 14 June 2024; Received in revised form 13 August 2024; Accepted 14 August 2024
Available online 21 August 2024

egg and the central cell. This fusion initiate embryo and endosperm development, marking the inception of seed formation (Baillie et al., 2023; Dresselhaus et al., 2016; Higashiyama and Takeuchi, 2015; Pereira et al., 2021).

From the development of male and female gametophytes up to double fertilization and seed development initiation, several signalling processes occur between different cells. Cell walls play an important role in this process, being involved in sensing the extracellular environment and transducing this information to the interior of the cell (Wolf, 2022). Despite many studies on the mechanisms of cell wall perception, the molecular players involved and how the signals are transduced and integrated inside the cell, remain unknown. The hydroxyproline (Hyp)-rich glycoprotein (HRGP) superfamily is the main class of cell surface glycoproteins in plants. The arabinogalactan-proteins (AGPs) are an important family belonging to this group and are involved in different stages of the reproductive process, from the formation of male and female gametophytes up to double fertilization and seed development (Acosta-García and Vielle-Calzada, 2004; Coimbra et al., 2009; Ellis et al., 2010; Li et al., 2010; Tan et al., 2012; Demesa-Arévalo and Vielle-Calzada, 2013; Pereira et al., 2014; Mizukami et al., 2016; Pereira et al., 2016; Leszczuk et al., 2019; Moreira et al., 2022). AGPs are highly glycosylated proteins decorated by arabinogalactan (AG) side chains containing arabinose, L-rhamnose, L-fucose, D-glucosamine, D-mannose, D-xylose, D-glucose, D-glucuronic acid, and D-galacturonic acid representing 90 % of the AGP molecule (Ellis et al., 2010; Hijazi et al., 2014; Showalter, 2001). Most of the AGPs are predicted to attach to the outer leaflet of the plasma membrane by a glycosylphosphatidylinositol (GPI) anchor. All these characteristics led to the study of these proteins as crucial players in the developmental and reproductive processes of angiosperms. AGP14, AGP18, and AGP22 play indispensable roles in the development of the FG (Acosta-García and Vielle-Calzada, 2004; Demesa-Arévalo and Vielle-Calzada, 2013; Tucker et al., 2012; Tucker and Koltunow, 2014), while AGP6, AGP11, AGP23, AGP40, FLA3 and FLA14 are specific to pollen and are involved in microspore development, and are crucial for correct PG germination (Da Costa et al., 2013; Miao et al., 2021; Pereira et al., 2016; Pereira et al., 2016). Additionally, early nodulin-proteins (ENODLs 11–15), which are chimeric AGPs, are known to control PT reception (Hou et al., 2016). AGP4/JAGGER is another important AGP, contributing to the persistent synergid cell degeneration and the cessation of PT attraction into the ovules (Pereira et al., 2016).

The study of AGPs over the years suggest that the protein core only serves as a molecular scaffold for the AG sugar chains, since these sugars account for more than 90 % of the entire molecule, so the functions of AGPs will be directly linked to glycosylation (Pennell et al., 1991; Seifert and Roberts, 2007; Silva et al., 2020). Furthermore, it is known that the attachment of sugar chains influences the localization, intracellular distribution, and stability of AGPs and most likely their ability to interact with other molecules (Leszczuk et al., 2023; Seifert and Roberts, 2007; Showalter, 2001). The addition of type-II AGs to the AGPs core protein is performed by 22 glycosyltransferases (GTs) (Silva et al., 2020). The process of glycosylation is initiated by the attachment of the first galactose residue to the hydroxyl group of hydroxyproline (Hyp) in the AGP backbone. This enzymatic reaction is catalyzed by galactosyltransferases known as Hyp-*O*-GALTs, specifically eight Hyp-GALTs - GALT2–6 & HPGT1–3 or GALT7–9 (Basu et al., 2015b, 2015a, 2013; Ogawa-Ohnishi and Matsubayashi, 2015; Showalter and Basu, 2016). Recently, by using reverse genetics, we showed defects in vegetative development and in reproductive processes, namely, in pollen and ovule development, seed morphology, and pollen-pistil interactions in multiple knockout mutants of the genes encoding these enzymes (Kaur et al., 2022, 2021; Moreira et al., 2023; Zhang et al., 2021). We demonstrated the crucial role of the AG polysaccharides in the reproductive processes using a quintuple knockout mutant (*galt25789*) (Kaur et al., 2022, 2021; Moreira et al., 2023). More recently, a more extreme higher-order mutant (*galt23456789 or 23456789*) revealed dramatically reduced seed-set and defects in male tissues, namely, exine, tectum patterning and intine thickness and low pollen viability (Kaur et al., 2023). A reduction in number of ovules in the *23456789* octuple mutants was also reported.

In this work, we complement and extend these previous studies by demonstrating the crucial role of these eight enzymes in the development of female reproductive tissues, by further studying the *23456789* octuple mutant. This octuple mutant reveals a higher quantity of unfertilized ovules which display abnormal callose accumulation both at the micropyle and, in some cases, throughout the entire embryo sac, when compared to the quintuple mutant. Additionally, the octuple mutant demonstrates the presence of ovules exhibiting abnormal embryo sac development, a reduction in glucuronic acid levels, and a disrupted spatiotemporal distribution of AGPs in the female tissues. These abnormalities ultimately result in impaired interactions between PTs and pistil tissues, leading to reduced seed formation and the development of defective embryos.

2. Material and methods

2.1. Plant material and growth conditions

A. thaliana (Columbia-0 ecotype) was obtained from the Arabidopsis Biological Research Center (ABRC), Columbus, Ohio, USA and used as wild-type (WT). The *23456789* mutants were generated as described previously (Kaur et al., 2023). The pAGP24:GUS constructs were generated and used to produce transgenic plants as described previously (Moreira et al., 2022). All plants used in this study were germinated after four days of stratification in the dark at 4°C and were grown in soil under long-day conditions (16 h of light/8 h of dark, 22°C, 60–70 % relative humidity) in plant growth chambers at a light intensity of 122 µmol m-2 s-1.

2.2. Seed set evaluation

Mature siliques were harvested from five-week-old plants and dissected to identify unfertilized ovules and matures seeds. The siliques at maturity were examined under a stereomicroscope (Model C-DSD230, Nikon).

2.3. Preparation of live plant material for microscopy

For reciprocal crosses, floral buds at stage 12 (Smyth et al., 1990) were emasculated before hand-pollination. Pistils were observed at stage 13/14 (Smyth et al., 1990) or 24–48 h after pollination (HAP) and dissected under a stereomicroscope (Model C-DSD230, Nikon) using hypodermic needles (0.4 ×20 mm; Braun). The opened carpels and the ovules that remained attached to the septum were maintained in mounting medium and covered with a coverslip.

2.4. Staining of pollen tubes with aniline blue

Arabidopsis flowers were fixed in 10 % (v/v) acetic acid and ethanol for 16 h at 4ºC, followed by three washes with water (5 min each) and bleaching with 1 M NaOH 8 N for 16 h, at 4ºC. After the 16 h, three washes were carried out again with water (30 min - 1 h each), and the material was incubated in a solution of decolorized aniline blue (DAB) (Mori et al., 2006) 0.1 % (w/v) for 16 h at 4ºC. Samples were observed using an inverted microscope (Eclipse Ti-S; Nikon) with UV fluorescence, and images were captured using a DS-Ri2 camera (Nikon).

2.5. Detection of GUS activity

GUS assays were performed on inflorescences as described by Liljegren et al. (2000), overnight. After chemical GUS detection, samples were incubated in clearing solution [160 g of chloral hydrate

(Sigma-Aldrich), 100 ml of water, and 50 ml of glycerol] and incubated at 4°C overnight. After that, flowers resulting from crosses between *23456789* pistils and pAGP24:GUS PGs (Moreira et al., 2022), together with flowers from pAGP24:GUS plants (WT background) were dissected under a stereomicroscope (model C-DSD230; Nikon) and observed under the microscope. A Zeiss AxioImager AZ microscope equipped with differential interference contrast optics was used. Images were captured with a ZeissAxiocam MRc3 camera using Zen Imaging Software (Zen 2011 SP1).

2.6. Seed size and width analysis

Approximately 50 Arabidopsis seeds were viewed in a Nikon Eclipse E600 microscope and photographed. Seed length and width was measured using ImageJ analysis software (https://imagej.nih.gov/ij/index.html), according to the instructions.

2.7. Ruthenium red staining

WT and *23456789* seeds were pre-hydrated in water for 1 h with shaking (200 rpm) to remove non-adherent mucilage and stained with 0.01 % ruthenium red for 30 min as previously described (Kaur et al., 2021). Ruthenium red stained seeds were examined under a Nikon SMZ1500 stereomicroscope coupled with a CCD Infinity 2 camera.

2.8. Plant material and light microscopy

Individual flowers from inflorescences of *A. thaliana* in stages 14–15 (Smyth et al., 1990) were fixed in 2 % (w/v) paraformaldehyde and 2.5 % (w/v) glutaraldehyde in PIPES buffer [0025 M, pH 7, 0.001 % (v/v) Tween-80], placed under vacuum for 1 h and then left at 4ºC overnight. After dehydration in a graded ethanol series, the material was embedded in LR White resin. Thick sections (0.7 mm) were obtained with a Leica EM UC7 Ultramicrotome, placed on glass slides and stained with a solution of 1 % (w/v) toluidine blue (Sigma-Aldrich, St Louis, MO, USA). Various slides were left unstained for immunolocalization with mAbs against AGP epitopes. Sections for brightfield microscopy were mounted with Eukitt quick-hardener (Fluka), and observations were made on a Zeiss AxioImager AZ microscope. Images were acquired with a Zeiss Axiocam MRc3 camera using Zen Imaging software (Zen 2011 SP1).

For phenotypic characterization, ovules at different stages of development (Smyth et al., 1990) were cleared with chloral hydrate and analysed as described previously (Brambilla et al., 2007). Samples were observed using a Zeiss AxioImager AZ microscope equipped with differential interference contrast lenses. Images were acquired with a Zeiss Axiocam MRc3 camera and processed with Zen Imaging software (Zen 2011 SP1). For characterization of embryo development, ovules at different stages of development were cleared with Visikol and a saturated solution of gum arabic (v:v). The samples were observed in a Nikon Eclipse E600 microscope equipped with a differential interference contrast (DIC) setting.

2.9. Immunolocalization and antibodies used

The following mAbs against AGPs were used: JIM8 (Pennell et al., 1991), JIM13 (Knox et al., 1991) and LM2 (Smallwood et al., 1996). Fluorescein isothiocyanate (FITC)-conjugated anti-rat IgG (Sigma-Aldrich F-1763) was used as secondary antibody. In slides prepared for immunolocalization, sections were treated as follows: 5 min in phosphate-buffered saline (PBS), pH 7.4, containing 5 % (w/v) non-fat dried milk (blocking solution), followed by incubation with primary antibody (diluted 1:5 in blocking solution), for 2 h at room temperature followed by overnight at 4ºC. After washing with PBS, sections were incubated with secondary antibody (diluted 1:100 in blocking solution) for 4 h in the dark, and finally washed with PBS followed by distilled water. Slides were further stained with 0.01 % (w/v) calcofluor white (Fluorescent Brightener 28; Sigma-Aldrich F3543) and mounted with Vectashield mounting medium (Vector Laboratories, Burlingame, CA, USA; ref: H-1000). Control experiments were performed omitting incubation with primary antibody (incubation with blocking solution only) and resulted in no staining with secondary antibody. Bright-field and fluorescence observations were performed on a Leica DMLB epifluorescence microscope [objectives were Leica N-Plan, and the filters used were 365/445 nm for calcofluor and 4',6-diamidino-2-phenylindole (DAPI); and 470/525 nm for the fluorescein stain]. Images were captured with a DS-Ri2 camera (Nikon) in automatic exposure mode and processed with Nikon NIS-Elements software. All images were processed for publication using ImageJ (Schneider et al., 2012).

2.10. Scanning electron microscopy

Seed samples were dry-mounted on aluminium stubs, covered by a 10 nm coat with palladium in a sputter coater (Anatech HUMMER 6.2 Sputtering System), and observed using a scanning electron microscope (SEM JEOL JSM-6390, HV/LV Tungsten/LaB6, Jeol USA Inc. 2012) equipped with an Energy Dispersive X-ray Spectroscopy (EDS) detector, with an accelerating voltage of 15 kV. Photographs were taken with SEM Control User Interface version 8.5 software at the Institute for Corrosion and Multiphase Technology, Ohio University. Both WT and *23456789* seeds were examined in three independent groups of approximately 20 seeds each.

2.11. Statistical analysis

All statistical analyses were conducted using GraphPad Prism version 8.0.2 for Windows (GraphPad Software, San Diego, CA, USA; www.graphpad.com, accessed on 24 August, 2023). Two-way analysis of variance and the post hoc Tukey test were applied to detect significant differences for all analysis, except for seed length and seed width, for this student's t-test was applied. The frequency of ovules with abnormal callose phenotype was calculated as the number of ovules with PT in the micropylar region and abnormal callose accumulation divided by the total number of ovules; and as the number of ovules without PT in the micropylar region, showing ectopic callose deposition in the whole embryo sac divided by the total number of ovules. The frequency of ovules with collapsed embryo sac (ES) was calculated as the number of ovules with collapsed ES in stage 14 divided by the total number of ovules observed.

3. Results

3.1. 23456789 mutant reveals significant reduction in seed set and higher rates of unfertilized ovules

Seed set of the octuple mutant, as previously reported in Kaur et al. (2023), was severely reduced (~86 %) when compared to the WT and the other Hyp-GALT mutants. In this work, the growth of WT and *23456789* plants was compared 40 days after germination. The examination of siliques in the *23456789* plants confirmed their reduced size compared to WT siliques and a visible reduction in the number of fully developed seeds, providing evidence of ovule abortion (Fig. 1 **A**). Quantification of unfertilized ovules revealed approximately 15 % (n=100 siliques) of the ovules were unfertilized in the mutant siliques (Fig. 1 **A**). The germination percentages of the *23456789* octuple mutants were significantly reduced by ~78 % compared to WT (Fig. 1**B-C**). Interestingly, it was determined that a longer stratification time could alleviate the reduced germination percentages (Supplemental Figure 1A**-D**) but could only improve the germination percentages to 46 % at the most (at 7d of imbibition).

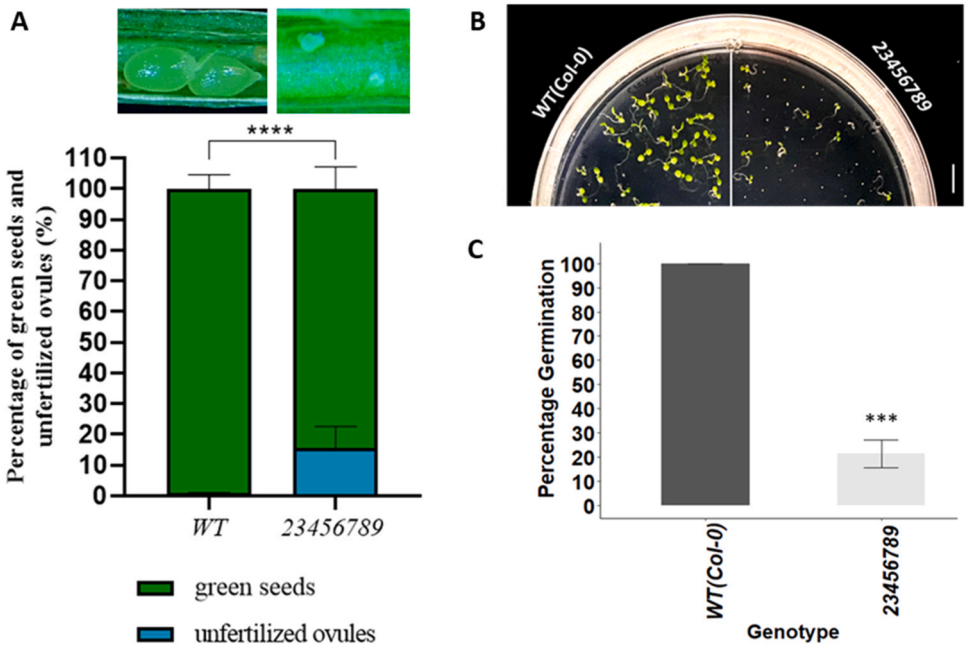

Fig. 1. ***23456789*** **plants showing a significant reduction in seed set and a higher percentage of unfertilized ovules. (A)** Percentages of green seeds and unfertilized ovules present in WT and *23456789* plants 40 days after germination (n = 100 siliques for each). On the top of the graphic: representative image of *23456789* green seeds (left) and *23456789* unfertilized ovules (right). **(B)** Germination of *23456789* seeds decreased in comparison to the WT. **(C)** Quantification of germinating seeds in *23456789* compared to WT. Germination percentages were examined 7 days after sowing (n = 28–30 seeds) in four independent experiments. Error bars denote mean standard deviation, **** above bars indicate significant differences between WT and *23456789* ($P \leq 0.0001$).

3.2. Pollen tube rupture defects in 23456789 plants

In vivo PT growth assays were performed in self-pollinated pistils from *23456789* and WT plants using DAB staining to detect callose in PTs. *23456789* self-pollinated pistils [stage 13/14 according to Smyth et al. (1990)] exhibited less PGs at the stigma surface when compared to the self-pollinated WT pistils, but subsequent pollen germination and PT growth along the pistil tissues appeared to proceed normally as in WT pistils (Figs. 2**A and** 2**C).** When visualizing PT arrival at the entrance of *23456789* ovules, abnormal callose accumulation was observed at the micropylar region of the embryo sac and ovule integuments in the presence of PTs (Fig. 2**D-E**). In addition, excessive callose accumulation was observed along the entire embryo sac in some ovules with no PTs growing towards them (Fig. 2**F**). While in WT ovules, PT arrival at the embryo sac entrance occurred normally with no callose deposition in this region (Fig. 2**B**).

Reciprocal crosses between WT and *23456789* plants were performed, and PT growth examined in the corresponding pistils by DAB staining. It was observed that the loss of these 8 *GALTs* in the FG is responsible for the observed callose accumulation in the embryo sacs (Fig. 3**A-C**). Moreover, not even the *GALTs* present in the growing WT PTs could rescue this phenotype, since the number of ovules with abnormal callose accumulation was similar in both self-pollinated *23456789* pistils and ♀ *23456789* × ♂ WT crosses (Fig. 3**F**). The *GALTs* in the male gametophyte seem to be dispensable for normal PT reception by the embryo sacs but are essential for PG germination and PT growth along the pistil tissues as demonstrated by the ♀ WT × ♂ *23456789* crosses (Fig. 3**D-E**). Additionally, in emasculated *23456789* and WT pistils, abnormal callose accumulation was almost undetected in either case (Supplemental Figure 2), indicating that this callose deposition in *GALT* deficient mutants is dependent on pollen-pistil interactions.

Either in self-pollinated *23456789* pistils or *23456789* pistils pollinated with wild type PGs, two distinct phenotypes regarding callose deposition were observed and quantified in the ovules: i) callose accumulation at the micropylar region of the ovule, in the embryo sac and integuments (Fig. 2**D-E** and Fig. 3**C**) (21 %, n=400 in self-pollinated *23456789* pistils; 19 %, n=200 in ♀ *23456789* × ♂ WT crosses) and ii) callose accumulation throughout the whole embryo sac (Fig. 2**F** and Fig. 3**B**) (9 %, n=400 in self-pollinated *23456789* pistils; 13 %, n=200 in ♀ *23456789* × ♂ WT crosses), which was virtually absent in the WT self-pollinated pistils and WT pistils pollinated with *23456789* PGs (Fig. 3**F-G**).

Controlled crosses between *23456789* pistils and a PG and PT marker line (pAGP24:GUS, Moreira et al., 2022) were performed to determine whether PT reception at the embryo sac was normal. In ♀ WT × ♂ pAGP24:GUS crosses, *GUS* expression was detected inside the whole embryo sac due to PT rupture and subsequent content release (Fig. 4**A**), but in ♀ *23456789* × ♂ pAGP24:GUS crosses, *GUS* expression was observed only inside the synergids, at the micropylar region of the embryo sac (Fig. 4**B**), suggesting a failure in PT rupture in these mutant ovules.

3.3. 23456789 defects in female gametophyte and ovule development

Analysis of cleared ovules from WT and *23456789* self-pollinated plants was performed to examine FG development and revealed the presence of abnormal embryo sacs in the octuple mutant. In several mutant ovules, embryo sac development was impaired, revealing collapsed embryo sacs (Fig. 5**B)** and abnormal embryo sacs with only one visible nucleus (Fig. 5**C**), when compared to WT ovules with normal embryo sacs (Fig. 5**A**). Ovules with developmental defects in embryo sacs were quantified in *23456789* self-pollinated pistils and approximately 27 % (n=400) of the ovules revealed compromised development of the embryo sac compared to only ~1 % (n=550) in WT (Fig. 5**D**). Furthermore, some ovules in the octuple mutant showed shorter inner integuments compared to WT (Supplemental Figure 3).

Sections of pistils from both *23456789* mutants and WT plants at stages 14 – 15 (Smyth et al., 1990) were embedded in LR-White resin and stained with toluidine blue to visualize ovule development in more detail. *23456789* ovules displayed a specific defect in their embryo sacs, namely the displacement of the embryo sac wall from the surrounding

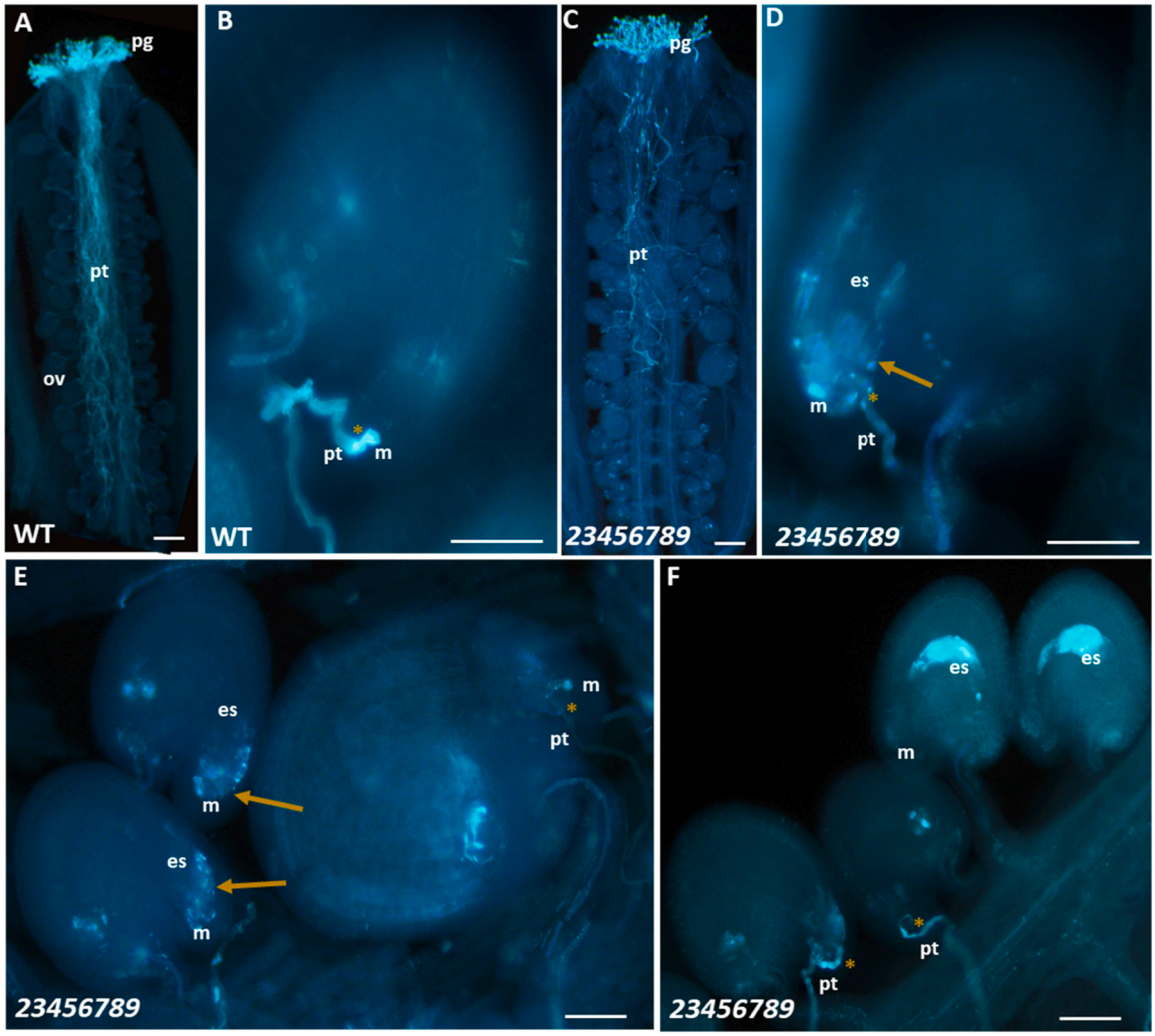

Fig. 2. Decolorized aniline blue staining of PTs in self-pollinated WT and *23456789* pistils. (A) PTs growing along the pistil tissues towards the entrance of the embryo sacs in a self-pollinated WT pistil. **(B)** Detail of a WT ovule with normal PT growth towards the embryo sac entrance and no abnormal callose accumulation. **(C)** Small number of PGs germinating at the surface of the stigma of a self-pollinated *23456789* pistil, with PTs growing towards the ovules. **(D)** Higher magnification of a *23456789* ovule displaying callose accumulation at the micropylar region of the ovule and its integuments (arrows). **(E)** Magnification of (**C**) showing unfertilized *23456789* ovules with callose accumulation at the micropylar end of the embryo sac (arrows) and a fertilized ovule. **(F)** Unfertilized *23456789* ovules with callose accumulation in the whole embryo sac. Yellow asterisks indicate the PT entering the embryo sac. es, embryo sac region; m, micropyle; ov, ovule; pg, pollen grain; pt, pollen tube; WT, wild-type. Scale bars: (A, C) = 100 μm; (B, D) = 20 μm; (E, F) = 50 μm.

cell layers and numerous small vacuoles in the central cell region (Fig. 5 **G – H**) in contrast to WT ovules (Fig. 5**E-F**).

3.4. Abnormal distribution of AGP epitopes inside unidentified structures in the embryo sac

Immunolocalization studies were carried out to visualize the distribution of AGP epitopes in the female tissues of the octuple mutant compared to WT. JIM8, an antibody used to recognize specific AGPs carbohydrate epitopes, was present in embryo sac walls, specifically in the micropylar region, at the filiform apparatus in WT and *23456789* female tissues **(**Fig. 6**A-B).** In addition, in octuple mutant ovules this antibody accumulated in small unidentified structures in the spaces created by the displacement of the embryo sac wall in the chalaza region (Fig. 6**B**). JIM13, another antibody used to recognize glycan epitopes from AGPs, labelled the embryo sac wall, its synergids and the filiform apparatus, as well as the inner integuments in WT and octuple mutant ovules (Fig. 6**C-D**). JIM13 also labelled small unidentified structures at the spaces created by the displacement of the octuple embryo sac wall in the chalaza and in small vacuoles near the central cell region (Fig. 6**D**). LM2, an antibody which recognizes glucuronic acid (GlcA) residues specific to AGPs, strongly labelled the ovules and ovary tissues in WT (Fig. 6**E**). In contrast, LM2 labelling was apparently reduced in the ovules and absent in the ovary tissues of the octuple mutant (Fig. 6**F**). LM2 also labelled small unidentified structures located outside the embryo sac wall and small vacuoles in the embryo sac near the central cell region (Fig. 6**F**).

3.5. 23456789 defects in embryo and seed development

Whole mount clearing allowed for observation of embryo development in *23456789* octuple mutants. Embryogenesis in WT seeds proceeds through a series of successive programmed stages: 1-cell, 2-cell, octant, globular, triangular, heart, and torpedo stages (Fig. 7**A**). However, in the octuple mutant, seeds with abnormal embryo development were observed within the same silique and these embryos were arrested at different stages of development (Fig. 7**B-C**). These embryo defects were seen between the one-cell and torpedo stages and were mostly related to abnormal cell divisions in the suspensor, the hypophysis and the apical region of the embryo. In Fig. 8**A-B**, bent cotyledon embryos

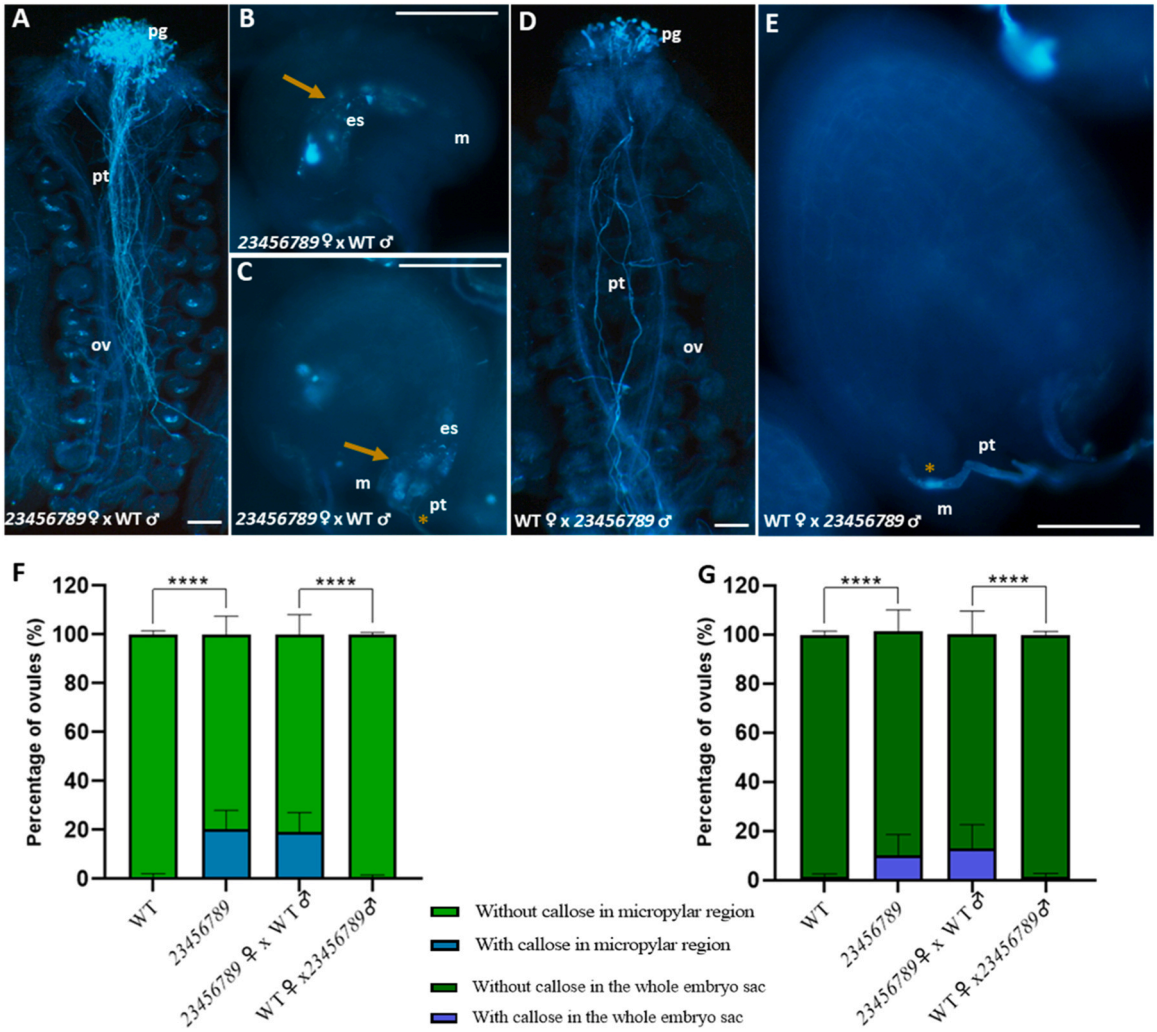

Fig. 3. Decolorized aniline blue staining of reciprocal crosses between WT and *23456789* plants and the observed frequency of different patterns of abnormal callose accumulation. (A-C) Aniline blue staining of reciprocal crosses between *23456789* pistils and WT PGs. **(A)** PGs germinating at the stigma and PTs growing towards the ovules. Some ovules show callose accumulation at the micropylar region of the embryo sac and in ovule integuments. **(B)** Unfertilized ovule with callose accumulation in the embryo sac. **(C)** PT entering the embryo sac with abnormal callose accumulation at the micropylar region (arrow). **(D-E)** Aniline blue staining of reciprocal crosses between WT pistils and *253456789* PGs. **(D)** PGs germinating at the surface of the stigma with some PTs growing along the pistil. **(E)** PT entering a normal ovule without ectopic callose accumulation. Yellow asterisks indicate the PT entering the embryo sac. **(F, G)** Quantitative analysis of ovules with an abnormal callose accumulation phenotype in the micropylar region and in whole embryo sac observed in self-pollinated WT and *23456789* pistils, and in reciprocal crosses between *23456789* and WT plants. WT, n = 550; *23456789*, n = 400; ♀ WT x ♂ *23456789*, n = 275; ♀ *23456789* x ♂ WT, n = 200. Values are expressed as percentages. Error bars denote mean ± standard deviation, **** above bars indicate significant differences between WT and *23456789* ($P \leq 0.0001$) and significant differences between ♀ WT x ♂ *23456789* and ♀ *23456789* x ♂ WT ($P \leq 0.001$). es, embryo sac region; m, micropyle; ov, ovule; pg, pollen grain; pt, pollen tube; WT, wild-type. Scale bars: (A, D) = 100 μm; (B, C) = 50 μm; (E) = 20 μm.

dissected from the octuple mutants and WT seeds were likely smaller in the octuple mutant seeds compared to WT. Indeed, octuple mutant seeds were abnormal and distorted with significantly lesser length and larger width (Fig. 8 **F-G**). Additionally, SEM seed morphology analysis revealed that the octuple mutant exhibited altered seed shape, but the seed coats surface looked similar (Fig. 8 **C-D**). To investigate the involvement of the Hyp-GALTs in modifying seed coat mucilage, ruthenium red staining, which stains acidic biopolymers such as pectin, was performed on the octuple mutant. A strong reduction in pectin staining in the mucilage adhering to the seeds was observed when compared to WT (Fig. 8**E**). Mutant ovules also showed reduced ruthenium red staining at the micropylar end (Supplemental Figure 4)**.**

4. Discussion

4.1. Under-glycosylation of AGPs impact male-female gametophyte interactions

The abnormal reproductive phenotypes of the *23456789* octuple mutant plants highlight the importance of GALT2–9 in male-female gametophyte interactions, consistent with previous findings (Moreira et al., 2023). We confirmed that seed set reduction in the octuple mutant (Kaur et al., 2023) is not only due to male gametophytic issues, but also due to a high rate of unfertilized ovules, likely a consequence of defective male – female gametophyte interactions. Additionally, low germination rates of octuple mutant seeds indicate redundant functions for these GALTs in seed germination.

Examination of *in vivo* PT growth in *23456789* self-pollinated pistils revealed two phenotypes: 1) abnormal callose accumulation at the ovule micropylar region, with PTs approaching this region, resembling the

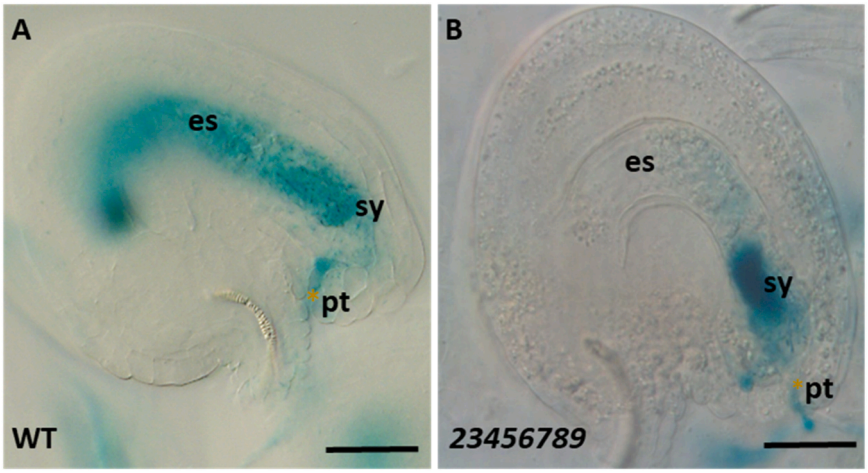

Fig. 4. Histochemical localization of GUS activity in WT and *23456789* ovules from pistils pollinated with pollen grains expressing the *pAGP24:GUS* fusion gene 24–48 HAP. (A) GUS activity driven by the *AGP24* promoter is detected in the PT and in the whole embryo sac of a WT ovule after normal PT rupture; **(B)** GUS activity driven by the *AGP24* promoter observed in the PT arriving at the embryo sac, and GUS activity detected at the micropylar region of the embryo sac after PT entrance in the region corresponding to the synergids. es, embryo sac region; pt, pollen tube; sy, synergid. Scale bars: (A – B) = 20 μm.

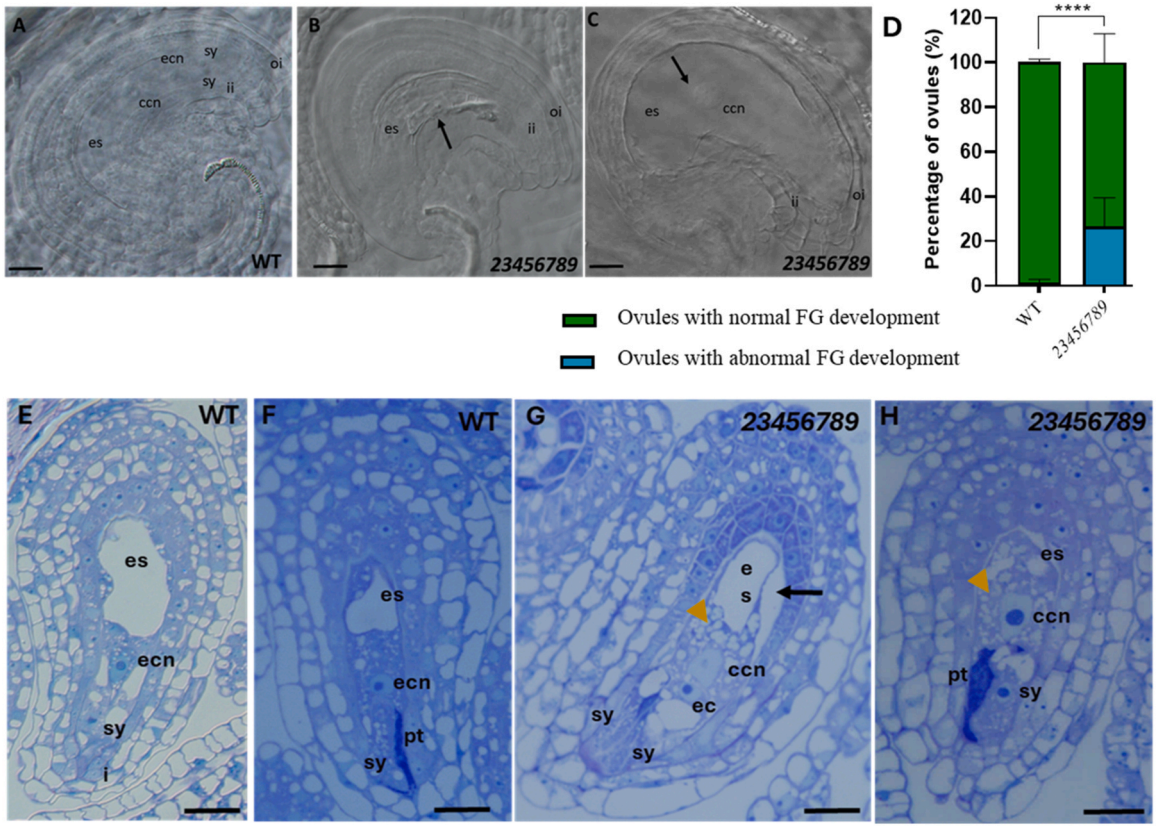

Fig. 5. Defects in female gametophyte and ovule development of *23456789* plants compared to WT. A-D. Cleared whole mount ovules of self-pollinated WT and *23456789* pistils**. (A)** WT ovule at FG6 stage (Drews et al., 1998) with one central cell (ccn), one egg cell (ecn) and two synergid cells (sy). **(B)** *23456789* ovule with a collapsed embryo sac (arrow). **(C)** *23456789* ovule with only one visible nucleus inside the embryo sac (arrow). **(D)** Quantitative analysis of ovules with collapsed embryo sac observed in self-pollinated WT and *23456789* pistils. WT, n = 550; *23456789*, n = 400. Values are expressed as percentages. Error bars denote mean ± standard deviation, **** indicate significant differences between WT and *23456789* ($P \leq 0.0001$). **E-H.** Cross sections of LR-White embedded ovules from *23456789* and WT plants stained with toluidine blue. **(E)** WT ovule showing normal development of the female gametophytic cells and integuments. **(F)** WT ovule showing pollen tube entering one of the synergids. **(G)** *23456789* ovules showing defects such as displacement of the embryo sac wall from the surrounding tissues (black arrow) and numerous small vacuoles in the central cell region (yellow triangle). **(H)** *23456789* ovules showing a pollen tube entering one of the synergids. ccn, central cell nucleus; ecn, egg cell nucleus; ec, egg cell; es, embryo sac region; fa, filiform apparatus; FG, female gametophyte; i, integument; ii, inner integument; oi, outer integuments; sy, synergids, WT, wild-type. Scale bars: (A – H) = 20 μm.

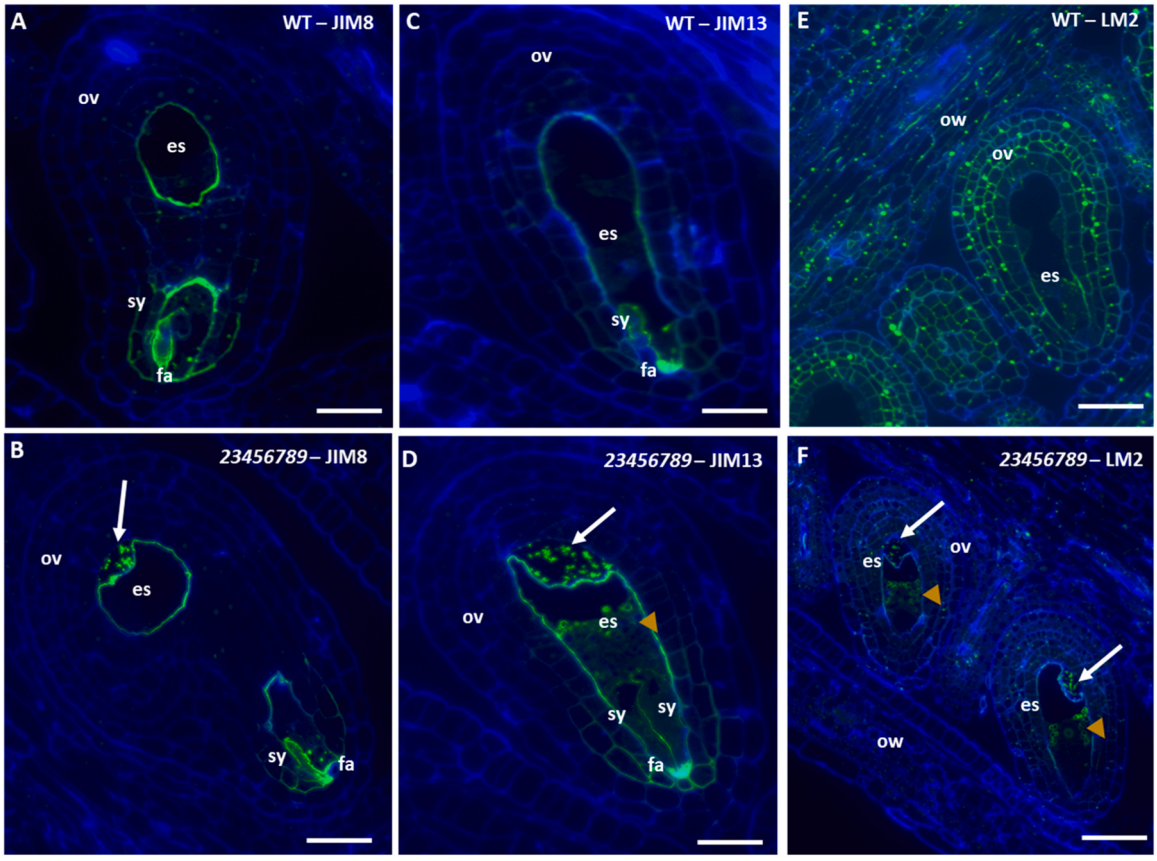

Fig. 6. Immunolocalization of AGPs recognized by the JIM8, JIM13 and LM2 antibodies in WT and *23456789* ovules. (A, B) Immunolocalization of the JIM8 epitope in WT (A) and *23456789* (B) ovules. **(A)** JIM8 labelled the embryo sac wall and the synergid cells, as well as the filiform apparatus. The integuments surrounding the embryo sac were also labelled by JIM8. **(B)** The JIM8 labelling signal in *23456789* ovules was strong in the embryo sac wall and filiform apparatus. The embryo sac was displaced from the surrounding tissues; JIM8 also labelled small unidentified structures outside the embryo sac wall (arrow). **(C, D)** Immunolocalization of the JIM13 epitope in WT (C) and *23456789* (D) ovules. **(C)** The embryo sac, the synergid filiform apparatus, and the inner integuments were strongly labelled by JIM13. **(D)** The embryo sac wall, the integuments, the synergids, and the filiform apparatus were strongly labelled by JIM13. The *23456789* embryo sac was displaced from the surrounding tissues with small vacuoles labelled with JIM13 near the central cell region (yellow triangle). JIM13 also labelled small unidentified structures outside the embryo sac wall (arrow). **(E, F)** Immunolocalization of the LM2 epitope in WT (E) and *23456789* (F) ovules. LM2 recognizes glucuronic acid (GlcA) residues in AGPs. **(E)** Strong LM2 labelling at the WT ovules and the ovary walls. **(F)** In the mutant, LM2 labelling was visible only in the ovules and was much weaker than in WT. Ovary walls were not labelled in the mutant. The *23456789* embryo sac was displaced from the ovule with small vacuoles showing LM2 labelling (yellow triangle). LM2 also labelled small unidentified structures outside the embryo sac wall (arrow).es, embryo sac region; fa, filiform apparatus; i, integument; ow, ovary wall; ov, ovule; WT, wild-type. Scale bar: (E,F) = 50 μm; (A-D) = 20 μm.

25789 phenotype (Moreira et al., 2023) and 2) abnormal callose accumulation in the whole embryo sac, with no PTs reaching the ovule. Reciprocal crosses with WT plants confirmed that these callose phenotypes were caused by the lack of the eight GALTs in the female tissues. Callose plays an important role in FG early development, disappearing when the embryo sac matures (Newbigin et al., 2009; Zhou et al., 2016; Zhou, 2019), and its presence at later stages of development indicates ovule abortion (Vishnyakova MA 1991; Sun et al., 2004). Inappropriate callose accumulation in this region may impair PT reception by the FG (Moreira et al., 2023). We demonstrated that in *23456789* pistils, PT burst fails in some *23456789* ovules, probably leading to abnormal callose accumulation at the micropylar region, as previously suggested (Moreira et al., 2023). Similar phenotypes were observed in mutants for other genes essential for the reproductive processes (Huck et al., 2003; Escobar-Restrepo et al., 2007; Liu et al., 2016; Duan et al., 2020; Ju et al., 2021). Furthermore, RNAi mutants for the chimeric AGPs ENODL13/14/15, early nodulin-like proteins with an arabinogalactan glycomodule and a GPI motif, exhibit callose deposition in the embryo sac as a defence response to PT overgrowth or structural collapse after fertilization failure (Hou et al., 2016).

Several AGPs are expressed in Arabidopsis female tissues (Moreira et al., 2022; Pereira et al., 2016; Pereira et al., 2014). AGP24, a classical AGP, is found in the functional megaspore, mature ovule embryo sacs before and after fertilization, immature seeds, and PGs, indicating its role in PT-embryo sac interactions (Moreira et al., 2022; Tucker and Koltunow, 2014). JAGGER/AGP4, another female specific AGP is involved in persistent synergid cell degeneration and polyspermy block (Pereira et al., 2016b). When compared to the quintuple mutant (Moreira et al., 2023), the octuple mutant has even more under-glycosylated AGPs, leading to their functional failure, which may explain the callose phenotype in the micropylar region upon PT arrival. Moreover, reduced de-esterified pectins, indicated by ruthenium red staining in *23456789* mutant ovules, suggests compromised PT-embryo sac interactions. Recently, a *feronia* mutant was shown to maintain de-esterified pectin at the filiform apparatus on the micropylar end for PT entrance (Duan et al., 2020). Similar reductions in ruthenium red staining were found in *glcat14a/b/c* mutants (Ajayi et al., 2022). Thus, we suggest that AGP carbohydrates and their interaction with other cell wall components like pectins are crucial for specific AGP functions in FG development and successful PT reception.

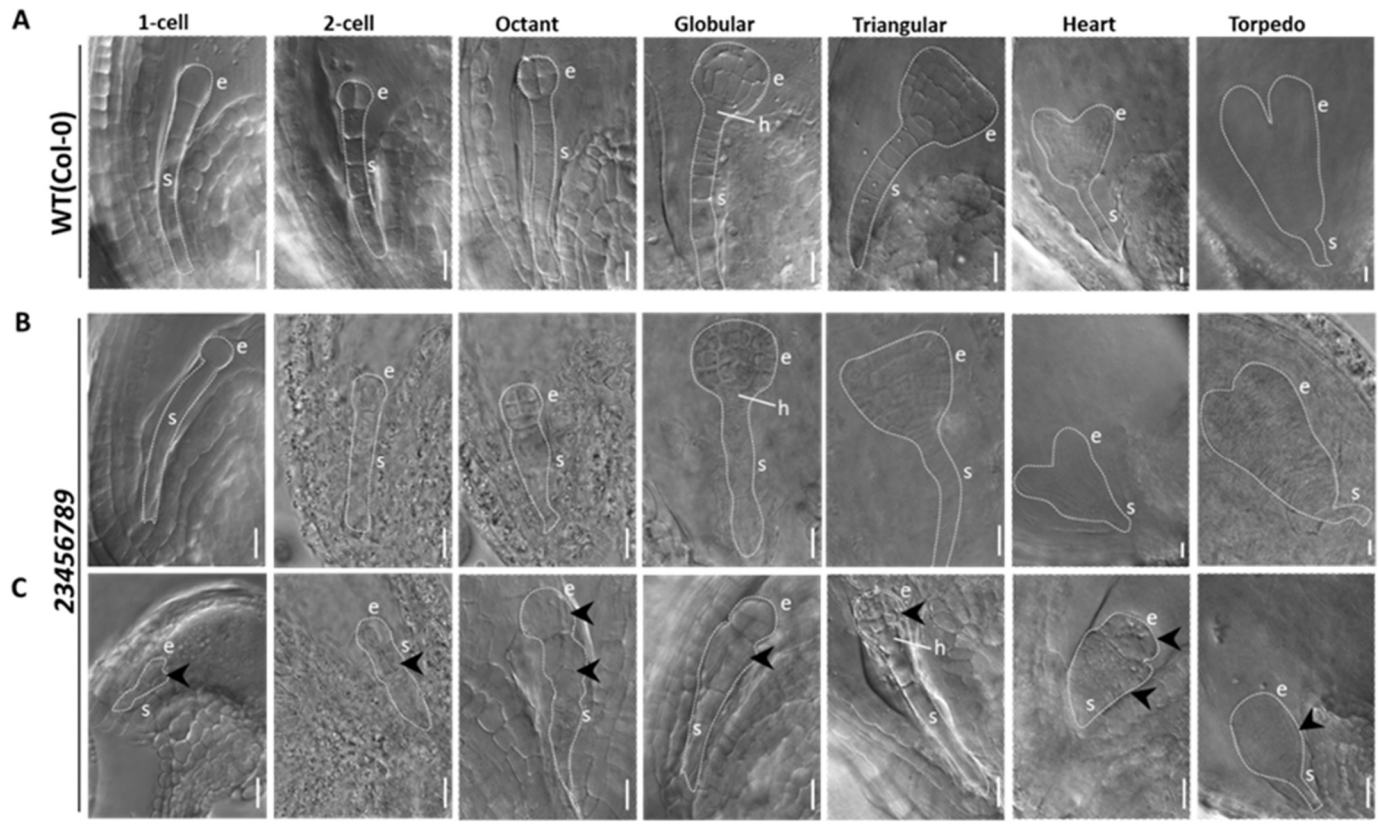

Fig. 7. Impaired embryo development in the ovules of *23456789* octuple mutants. The developmental stages of embryogenesis from 1-cell to torpedo stage were defined according to Wendrich and Weijers (2013). **(A)** Normally developing embryos at the 1-cell, 2-cell, octant, globular, triangular, heart and torpedo stages in WT. **(B)** and **(C)** represents *23456789* octuple mutant embryos. **(B)** shows normal embryo development in the octuple mutant. Octuple mutant embryos also had developmental defects with abnormal divisions in the suspensor/ hypophysis and/or in the embryo itself (~10 %) as indicated by black arrows in **(C)**. Black arrows point towards the defective divisions occurring in the embryo or suspensor leading to abnormal shapes and hence, their developmental arrest. White dashed lines in the figure panels are marked to help visualize embryo development. Embryo shapes were visualized after Visikol treatment (n>150 embryos). e, embryo; h, hypophysis; s, suspensor. Scale bars = 100 μm.

4.2. The lack of GALT2-9 affects female gametophyte and embryo development

The functional loss of eight Hyp-GALTs (GALT2–9) compromises FG development. Detailed analysis of the *23456789* mutant revealed abnormal embryo sac development in a considerable number of cases, probably related to ovules exhibiting ectopic callose accumulation throughout the embryo sac, without fertilization. Callose is known for its barrier functions in isolating dead or dysfunctional cells (Sun et al., 2004), suggesting these ovules collapse due to abnormal development. Furthermore, some mutant ovules revealed shorter inner integuments compared to WT as in *galt25789* mutant (Moreira et al., 2023), potentially affecting FG development. Several *23456789* ovules also exhibited partial displacement of the embryo sac wall from surrounding cell layers and accumulated small unidentified structures immuno-labelled for AGP sugar epitopes, indicating modified AGPs spatiotemporal distribution in the embryo sac, likely due to defective glycosylation.

AGPs function as molecular determinants for female reproductive development, being crucial for cell wall modification and cell differentiation in reproductive tissues (Lopes et al., 2023). They accumulate specifically in the FG cell walls and in the nucellar epidermis during early ovule development (Coimbra et al., 2007; Tucker and Koltunow, 2014), suggesting a role in FG development. Specific AGPs including *AGP22* and *AGP24* are expressed in the FG and nucellus cells (Tucker et al. 2012; Moreira et al., 2022), and AGP18 is critical for functional megaspore development in Arabidopsis (Demesa-Arévalo and Vielle-Calzada, 2013). AGP18 is transcribed in the ovule somatic tissues and moves to the functional megaspore to be translated, where it is glycosylated, indicating the importance of glycosylation for its function here (Demesa-Arévalo and Vielle-Calzada, 2013). Thus, most probably, the lack of these eight GALTs leads to the under-glycosylation of AGPs essential for FG development.

The octuple mutant also shows defects during embryo development. Immunolocalization studies detected AGPs at different embryo development stages suggesting its involvement in embryogenesis (McCabe et al., 1997; Pennell et al., 1991; Pérez-Pérez et al., 2019; Seifert and Roberts, 2007; Van Hengel et al., 2002; Zhong et al., 2011). Besides being fundamental for embryo development, the lack of the GALTs also result in defects in seed shape, size and germination, and reduced adherent mucilage extruded upon seed hydration. These defects are more exaggerated than those observed in the *galt25789* quintuple mutant (Kaur et al., 2021). AGPs, although a small part of the seed mucilage, are important for deposition of cellulose rays in the seed coat mucilage (Griffiths et al., 2016). AGP glucuronosyltransferase mutants revealed by immunolabelling and biochemical analyses that GlcA sugars on AGPs are essential for pectin and cellulose matrix organization in Arabidopsis seed coat mucilage (Ajayi et al., 2021; Zhang et al., 2020). AGP glycosylation likely maintains seed shape and mucilage production, by interacting with other mucilage components such as pectins (Kaur et al., 2021).

4.3. 23456789 reveals a low glucuronic acid content in female tissues

23456789 ovules demonstrated an apparent reduction in labeling with LM2, an antibody recognizing AGP carbohydrate epitopes containing β-linked GlcA, and an absence of labeling in the ovary walls, as

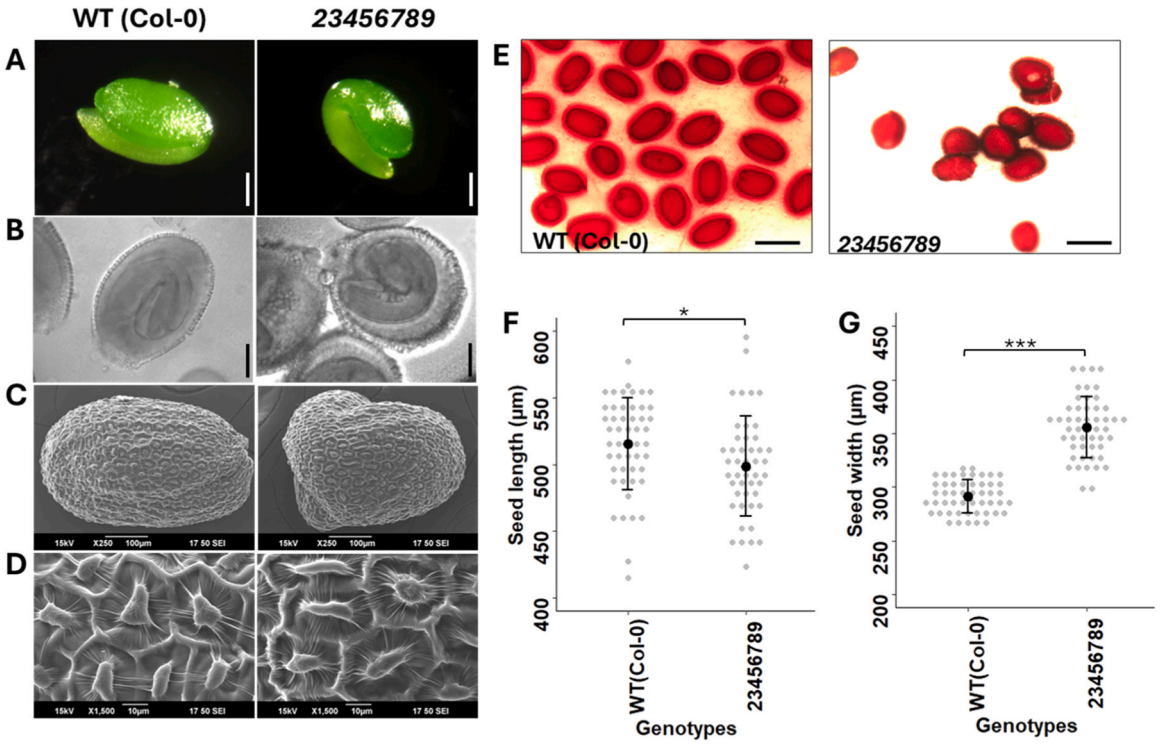

Fig. 8. Microscopic analysis of mature embryos and seeds and ruthenium red staining of seed coat mucilage from WT and *23456789* mutant plants. (A) WT and *23456789* bent mature embryos removed from the seeds and observed under the stereomicroscope. The *23456789* octuple mutant displayed an abnormal shape of the mature embryo in comparison to the normal, oblong shape of WT mature embryos. **(B)** DIC microscopy images of cleared mature embryos from WT and *23456789* mutant seeds showing the abnormal mature embryos in the mutant. **(C)** Dry seeds imaged by SEM. Like the mature embryos, the seeds of the *23456789* octuple mutants were abnormal and wider in shape. **(D)** The detailed surface morphology of dry mature Arabidopsis WT and *23456789* seeds visualized by SEM. **(E)** Staining of seed coat mucilage with ruthenium red (for pectin) following the removal of the outer mucilage. (**F and G**) Seed length and seed width of WT and *23456789* mutants (mean ± SD, n=50). * P <0.05, *** P <0.001. Scale bars (A and B) = 100 µm.

observed in the *galt25789* mutant (Kaur et al., 2021; Moreira et al., 2023). GlcA is added to β-1,3 and β-1,6-linked galactans of AG glycans by β-glucuronosyltransferases (GlcATs) (Dilokpimol et al. 2014; Lopez-Hernandez et al., 2020), an essential process for AGP biological functions, as GlcA residues enable AGPs to bind Ca^{2+} ions (Ajayi et al., 2022, 2021; Lamport and Várnai, 2013; Lopez-Hernandez et al., 2020). In *Torenia fournieri*, GlcA was identified as an essential component of the disaccharide AMOR, required for making PTs responsive to female attraction molecules, such as LURES (Mizukami et al., 2016). Recent studies showed that the mutants *glcat14a*, *glcat14b*, and *glcat14c*, part of the GT14 family of β-glucuronosyltransferases, presented developmental and reproductive defects due to a reduction in Ca^{2+}-AGP GlcA binding (Ajayi et al., 2021; Lopez-Hernandez et al., 2020; Zhang et al., 2020). Ca^{2+} oscillations are critical for many reproductive events in plants, suggesting that female and male specific AGPs might play a role in calcium-mediated signalling pathways (Iwano et al., 2012; Lamport, 2023; Lamport et al., 2021). We expected a reduction in all AGP epitopes analysed by immunocytochemistry. The fact that this did not occur suggests that other Hyp-GALTs are involved in adding the first galactose residue to AGPs, since the phenotypes observed are not fully penetrant.

5. Conclusions

This study emphasizes the important role of eight GALTs (GALT2–9) in AGP glycosylation in female tissues, extending our previous findings (Kaur et al., 2023, 2022; Moreira et al., 2023). Proper AGP glycosylation as initiated by these GALTs is essential for correct spatiotemporal distribution of AGPs which in turn is vital for female reproductive development, PT-embryo sac interactions, embryo and seed development. Our study supports the hypothesis that the initial sugar additions influence the terminal deposition of GlcA, demanding further biochemical investigations. The severe phenotypes observed with the loss of these Hyp-GALTs suggest their common contribution to AGP glycosylation and the existence of other enzymes performing this function, which remain to be identified.

Funding

This work received financial support from FCT/MCTES (UIDB/50006/2020 DOI 10.54499/UIDB/50006/2020) through national funds. DM's research was supported by an FCT PhD grant SFRH/BD/143557/2019. DK's work was supported by an Ohio University (OU) Student Enhancement Award; an OU College of Arts and Science Graduate Student Research Fund award; and an OU Nanoscale & Quantum Phenomena Institute (NQPI) fellowship to D.K. AMP and SC research was supported by EU project 101086293—CRISPit, funded by HORIZON-TMA-MSCA-SE.

CRediT authorship contribution statement

Ana Marta Pereira: Writing – review & editing, Validation, Supervision, Investigation, Funding acquisition, Formal analysis. **Sílvia Coimbra:** Writing – review & editing, Supervision, Funding acquisition, Formal analysis. **Sara Fourbert-Mendes:** Investigation. **Allan M. Showalter:** Writing – review & editing, Validation, Supervision, Formal analysis. **Diana Moreira:** Writing – review & editing, Writing – original draft, Validation, Methodology, Investigation, Funding acquisition, Formal analysis, Conceptualization. **Dasmeet Kaur:** Writing – review & editing, Writing – original draft, Methodology, Investigation, Funding acquisition, Formal analysis, Conceptualization.

Declaration of Competing Interest

The authors declare that they have no known competing financial interests or personal relationships that could have appeared to influence the work reported in this paper.

Data availability

Data will be made available on request.

Acknowledgment

This work received support and help from FCT/MCTES (LA/P/0008/2020 DOI 10.54499/LA/P/0008/2020, UIDP/50006/2020 DOI 10.54499/UIDP/50006/2020 and UIDB/50006/2020 DOI 10.54499/UIDB/50006/2020), through national funds. We thank Dr. Maria Martins (Faculty of Sciences, University of Porto) for help in statistical analysis. We thank Molecular and Cellular Biology program, Ohio University (OU) for providing the funds for biochemical experiments

Author contributions

DM designed the research, performed the experiments, analysed the data, and wrote the initial draft of the manuscript. DM conducted seed set analysis, decolorized aniline blue staining, reciprocal crosses, ovules whole mount clearing and immunolocalization analysis. DK wrote the subsequent drafts of the manuscript and conducted whole mount clearing technique for embryos, germination studies, seeds SEM and ruthenium red staining. SFM obtained ovules LR-White sections and performed the toluidine blue staining. AMS, SC and AMP conceived the study, helped to analyze and interpret the data, and were involved in reviewing and writing subsequent drafts of the manuscript. All authors have read and approved the manuscript.

Appendix A. Supporting information

Supplementary data associated with this article can be found in the online version at doi:10.1016/j.plantsci.2024.112231.

References

G. Acosta-García, J.P. Vielle-Calzada, A classical arabinogalactan protein is essential for the initiation of female gametogenesis in Arabidopsis, Plant Cell 16 (2004), https://doi.org/10.1105/tpc.104.024588.

O.O. Ajayi, M.A. Held, A.M. Showalter, Glucuronidation of type II arabinogalactan polysaccharides function in sexual reproduction of Arabidopsis, Plant J. 109 (2022) 164–181, https://doi.org/10.1111/tpj.15562.

O.O. Ajayi, M.A. Held, A.M. Showalter, Three β-glucuronosyltransferase genes involved in arabinogalactan biosynthesis function in Arabidopsis growth and development, Plants 10 (2021), https://doi.org/10.3390/plants10061172.

A.L. Baillie, J. Sloan, L.-J. Qu, L.M. Smith, Signalling between the sexes during pollen tube reception, Trends Plant Sci. (2023), https://doi.org/10.1016/j.tplants.2023.07.011.

D. Basu, Y. Liang, X. Liu, K. Himmeldirk, A. Faik, M. Kieliszewski, M. Held, A. M. Showalter, Functional identification of a hydroxyproline-O-galactosyltransferase specific for arabinogalactan protein biosynthesis in Arabidopsis, J. Biol. Chem. 288 (2013), https://doi.org/10.1074/jbc.M112.432609.

D. Basu, L. Tian, W. Wang, S. Bobbs, H. Herock, A. Travers, A.M. Showalter, A small multigene hydroxyproline-O-galactosyltransferase family functions in arabinogalactan-protein glycosylation, growth and development in Arabidopsis, BMC Plant Biol. 15 (2015a), https://doi.org/10.1186/s12870-015-0670-7.

D. Basu, W. Wang, S. Ma, T. DeBrosse, E. Poirier, K. Emch, E. Soukup, L. Tian, A. M. Showalter, Two hydroxyproline galactosyltransferases, GALT5 and GALT2, function in arabinogalactan-protein glycosylation, growth and development in Arabidopsis, PLoS One 10 (2015b), https://doi.org/10.1371/journal.pone.0125624.

V. Brambilla, R. Battaglia, M. Colombo, S. Masiero, S. Bencivenga, M.M. Kater, L. Colombo, Genetic and Molecular Interactions between BELL1 and MADS Box Factors Support Ovule Development in Arabidopsis, The Plant Cell 19 (2007) 2544–2556, https://doi.org/10.1105/tpc.107.051797.

S. Coimbra, J. Almeida, V. Junqueira, M.L. Costa, L.G. Pereira, Arabinogalactan proteins as molecular markers in *Arabidopsis thaliana* sexual reproduction, J. Exp. Bot. 58 (2007) 4027–4035, https://doi.org/10.1093/jxb/erm259.

S. Coimbra, M. Costa, B. Jones, M.A. Mendes, L.G. Pereira, Pollen grain development is compromised in Arabidopsis *agp6 agp11* null mutants, J. Exp. Bot. 60 (2009) 3133–3142, https://doi.org/10.1093/JXB/ERP148.

M. Colombo, S. Masiero, S. Vanzulli, P. Lardelli, M.M. Kater, L. Colombo, *AGL23*, a type I MADS-box gene that controls female gametophyte and embryo development in Arabidopsis, Plant J. 54 (2008) 1037–1048, https://doi.org/10.1111/j.1365-313X.2008.03485.x.

M.L. Da Costa, L.G. Pereira, S. Coimbra, Growth media induces variation in cell wall associated gene expression in *Arabidopsis thaliana* pollen tube, Plants 2013 Vol. 2 (429-440 2) (2013) 429–440, https://doi.org/10.3390/PLANTS2030429.

E. Demesa-Arévalo, J.P. Vielle-Calzada, The classical arabinogalactan protein AGP18 mediates megaspore selection in Arabidopsis, Plant Cell 25 (2013), https://doi.org/10.1105/tpc.112.106237.

A. Dilokpimol, C.P. Poulsen, G. Vereb, S. Kaneko, A. Schulz, N. Geshi, Galactosyltransferases from Arabidopsis thaliana in the biosynthesis of type II arabinogalactan: molecular interaction enhances enzyme activity, BMC Plant Biol. 14 (2014), https://doi.org/10.1186/1471-2229-14-90.

T. Dresselhaus, S. Sprunck, G.M. Wessel, Fertilization mechanisms in flowering plants, Curr. Biol. (2016), https://doi.org/10.1016/j.cub.2015.12.032.

G.N. Drews, D. Lee, C.A. Christensen, Genetic analysis of female gametophyte development and function, Plant Cell 10 (1998) 5–17, https://doi.org/10.1105/tpc.10.1.5.

G.N. Drews, R. Yadegari, Development and function of the angiosperm female gametophyte, Annu Rev. Genet 36 (2002) 99–124, https://doi.org/10.1146/annurev.genet.36.040102.131941.

Q. Duan, M.C.J. Liu, D. Kita, S.S. Jordan, F.L.J. Yeh, R. Yvon, H. Carpenter, A. N. Federico, L.E. Garcia-Valencia, S.J. Eyles, C.S. Wang, H.M. Wu, A.Y. Cheung, FERONIA controls pectin- and nitric oxide-mediated male–female interaction, Nature 579 (2020), https://doi.org/10.1038/s41586-020-2106-2.

M. Ellis, J. Egelund, C.J. Schultz, A. Bacic, Arabinogalactan-proteins: key regulators at the cell surface? Plant Physiol. 153 (2010) https://doi.org/10.1104/pp.110.156000.

J.M. Escobar-Restrepo, N. Huck, S. Kessler, V. Gagliardini, J. Gheyselinck, W.C. Yang, U. Grossniklaus, The Feronia receptor-like kinase mediates male-female interactions during pollen tube reception, Science 317 (2007) 1979, https://doi.org/10.1126/science.1143562.

J.S. Griffiths, M.-J. Crepeau, M.-C. Ralet, G.J. Seifert, H.M. North, Dissecting seed mucilage adherence mediated by FEI2 and SOS5, Front Plant Sci. 7 (2016), https://doi.org/10.3389/fpls.2016.01073.

T. Higashiyama, H. Takeuchi, The mechanism and key molecules involved in pollen tube guidance, Annu Rev. Plant Biol. 66 (2015), https://doi.org/10.1146/annurev-arplant-043014-115635.

M. Hijazi, S.M. Velasquez, E. Jamet, J.M. Estevez, C. Albenne, An update on post-translational modifications of hydroxyproline-rich glycoproteins: toward a model highlighting their contribution to plant cell wall architecture, Front Plant Sci. (2014), https://doi.org/10.3389/fpls.2014.00395.

Y. Hou, X. Guo, P. Cyprys, Y. Zhang, A. Bleckmann, L. Cai, Q. Huang, Y. Luo, H. Gu, T. Dresselhaus, J. Dong, L.J. Qu, Maternal ENODLs are required for pollen tube reception in arabidopsis, Curr. Biol. 26 (2016), https://doi.org/10.1016/j.cub.2016.06.053.

N. Huck, J.M. Moore, M. Federer, U. Grossniklaus, The Arabidopsis mutant *feronia* disrupts the female gametophytic control of pollen tube receptor. Development (2003) https://doi.org/10.1242/dev.00458.

M. Iwano, Q.A. Ngo, T. Entani, H. Shiba, T. Nagai, A. Miyawaki, A. Isogai, U. Grossniklaus, S. Takayama, Cytoplasmic Ca2+ changes dynamically during the interaction of the pollen tube with synergid cells, Development 139 (2012) 4202–4209, https://doi.org/10.1242/dev.081208.

Y. Ju, J. Yuan, D.S. Jones, W. Zhang, C.J. Staiger, S.A. Kessler, Polarized NORTIA accumulation in response to pollen tube arrival at synergids promotes fertilization, Dev. Cell 56 (2021), https://doi.org/10.1016/j.devcel.2021.09.026.

D. Kaur, M.A. Held, M.R. Smith, A.M. Showalter, Functional characterization of hydroxyproline-O-galactosyltransferases for Arabidopsis arabinogalactan-protein synthesis, BMC Plant Biol. 21 (2021) 590, https://doi.org/10.1186/s12870-021-03362-2.

D. Kaur, M.A. Held, Y. Zhang, D. Moreira, S. Coimbra, A.M. Showalter, Knockout of eight hydroxyproline-O-galactosyltransferases cause multiple vegetative and reproductive growth defects, Cell Surf. 10 (2023) 100117, https://doi.org/10.1016/j.tcsw.2023.100117.

D. Kaur, D. Moreira, S. Coimbra, A.M. Showalter, Hydroxyproline-O-Galactosyltransferases synthesizing type II arabinogalactans are essential for male gametophytic development in Arabidopsis, Front Plant Sci. 13 (2022), https://doi.org/10.3389/fpls.2022.935413.

J.P. Knox, P.J. Linstead, J.P.C. Cooper, K. Roberts, Developmentally regulated epitopes of cell surface arabinogalactan proteins and their relation to root tissue pattern formation, Plant J. 1 (1991), https://doi.org/10.1046/j.1365-313X.1991.t01-9-00999.x.

D.T.A. Lamport, The growth oscillator and plant stomata: an open and shut case, Plants 12 (2023) 2531, https://doi.org/10.3390/plants12132531.

D.T.A. Lamport, L. Tan, M.J. Kieliszewski, A molecular pinball machine of the plasma membrane regulates plant growth—a new paradigm, Cells (2021), https://doi.org/10.3390/cells10081935.

D.T.A. Lamport, P. Várnai, Periplasmic arabinogalactan glycoproteins act as a calcium capacitor that regulates plant growth and development, N. Phytol. 197 (2013) 58–64, https://doi.org/10.1111/nph.12005.

A. Leszczuk, P. Kalaitzis, J. Kulik, A. Zdunek, Review: structure and modifications of arabinogalactan proteins (AGPs), BMC Plant Biol. 23 (2023) 45, https://doi.org/10.1186/s12870-023-04066-5.

A. Leszczuk, E. Szczuka, A. Zdunek, Arabinogalactan proteins: Distribution during the development of male and female gametophytes, Plant Physiol. Biochem. 135 (2019) 9–18, https://doi.org/10.1016/j.plaphy.2018.11.023.
J. Li, M. Yu, L.L. Geng, J. Zhao, The fasciclin-like arabinogalactan protein gene, FLA3, is involved in microspore development of Arabidopsis, Plant J. 64 (2010), https://doi.org/10.1111/j.1365-313X.2010.04344.x.
S.J. Liljegren, G.S. Ditta, Y. Eshed, B. Savidge, J.L. Bowmant, M.F. Yanofsky, SHATTERPROOF MADS-box genes control seed dispersal in Arabidopsis, Nature 2000 404 (6779 404) (2000) 766–770, https://doi.org/10.1038/35008089.
X. Liu, C. Castro, Y. Wang, J. Noble, N. Ponvert, M. Bundy, C. Hoel, E. Shpak, R. Palanivelu, The role of LORELEI in pollen tube reception at the interface of the synergid cell and pollen tube requires the modified eight-cysteine motif and the receptor-like kinase FERONIA, Plant Cell 28 (2016), https://doi.org/10.1105/tpc.15.00703.
A.L. Lopes, D. Moreira, A.M. Pereira, R. Ferraz, S. Mendes, L.G. Pereira, L. Colombo, S. Coimbra, AGPs as molecular determinants of reproductive development, Ann. Bot. 131 (2023) 827–838, https://doi.org/10.1093/aob/mcad046.
F. Lopez-Hernandez, T. Tryfona, A. Rizza, X.L. Yu, M.O.B. Harris, A.A.R. Webb, T. Kotake, P. Dupree, Calcium binding by arabinogalactan polysaccharides is important for normal plant development, Plant Cell 32 (2020), https://doi.org/10.1105/tpc.20.00027.
P.F. McCabe, T.A. Valentine, L.S. Forsberg, R.I. Pennell, Soluble signals from cells identified at the cell wall establish a developmental pathway in carrot, Plant Cell 9 (1997) 2225, https://doi.org/10.2307/3870581.
Y. Miao, J. Cao, L. Huang, Y. Yu, S. Lin, FLA14 is required for pollen development and preventing premature pollen germination under high humidity in Arabidopsis, BMC Plant Biol. 21 (2021) 254, https://doi.org/10.1186/s12870-021-03038-x.
A.G. Mizukami, R. Inatsugi, J. Jiao, T. Kotake, K. Kuwata, K. Ootani, S. Okuda, S. Sankaranarayanan, Y. Sato, D. Maruyama, H. Iwai, E. Garénaux, C. Sato, K. Kitajima, Y. Tsumuraya, H. Mori, J. Yamaguchi, K. Itami, N. Sasaki, T. Higashiyama, The AMOR arabinogalactan sugar chain induces pollen-tube competency to respond to ovular guidance, Curr. Biol. 26 (2016), https://doi.org/10.1016/j.cub.2016.02.040.
D. Moreira, D. Kaur, A.M. Pereira, M.A. Held, A.M. Showalter, S. Coimbra, Type II arabinogalactans initiated by hydroxyproline-O-galactosyltransferases play important roles in pollen–pistil interactions, Plant J. 114 (2023) 371–389, https://doi.org/10.1111/tpj.16141.
D. Moreira, A.L. Lopes, J. Silva, M.J. Ferreira, S.C. Pinto, S. Mendes, L.G. Pereira, S. Coimbra, A.M. Pereira, New insights on the expression patterns of specific Arabinogalactan proteins in reproductive tissues of *Arabidopsis thaliana*, Front Plant Sci. 13 (2022), https://doi.org/10.3389/fpls.2022.1083098.
T. Mori, H. Kuroiwa, T. Higashiyama, T. Kuroiwa, Generative cell specific 1 is essential for angiosperm fertilization, Nat. Cell Biol. 8 (2006) 64–71, https://doi.org/10.1038/ncb1345.
Newbigin, E., Bacic, A., Read, S., 2009. Callose and its role in pollen and embryo sac development in flowering plants, in: Chemistry, Biochemistry, and Biology of 1-3 Beta Glucans and Related Polysaccharides. https://doi.org/10.1016/B978-0-12-373971-1.00014-5.
M. Ogawa-Ohnishi, Y. Matsubayashi, Identification of three potent hydroxyproline O-galactosyltransferases in Arabidopsis, Plant J. 81 (2015), https://doi.org/10.1111/tpj.12764.
R.I. Pennell, L. Janniche, P. Kjellbom, G.N. Scofield, J.M. Peart, K. Roberts, Developmental regulation of a plasma membrane arabinogalactan protein epitope in oilseed rape flowers, Plant Cell (1991), https://doi.org/10.1105/tpc.3.12.1317.
Ana M. Pereira, A.L. Lopes, S. Coimbra, Arabinogalactan proteins as interactors along the crosstalk between the pollen tube and the female tissues, Front Plant Sci. 7 (2016), https://doi.org/10.3389/fpls.2016.01895.
A.M. Pereira, S. Masiero, M.S. Nobre, M.L. Costa, M.T. Solís, P.S. Testillano, S. Sprunck, S. Coimbra, Differential expression patterns of arabinogalactan proteins in *Arabidopsis thaliana* reproductive tissues, J. Exp. Bot. 65 (2014) 5459–5471, https://doi.org/10.1093/JXB/ERU300.
A.M. Pereira, D. Moreira, S. Coimbra, S. Masiero, Paving the way for fertilization: The role of the transmitting tract, Int J. Mol. Sci. (2021), https://doi.org/10.3390/ijms22052603.
Ana Marta Pereira, M.S. Nobre, S.C. Pinto, A.L. Lopes, M.L. Costa, S. Masiero, S. Coimbra, love Is Strong, and You're so Sweet": JAGGER Is Essential for Persistent Synergid Degeneration and Polytubey Block in *Arabidopsis thaliana*, Mol. Plant 9 (2016), https://doi.org/10.1016/j.molp.2016.01.002.
Y. Pérez-Pérez, E. Carneros, E. Berenguer, M.-T. Solís, I. Bárány, B. Pintos, A. Gómez-Garay, M.C. Risueño, P.S. Testillano, Pectin De-methylesterification and AGP Increase Promote Cell Wall Remodeling and Are Required During Somatic Embryogenesis of *Quercus suber*, Front Plant Sci. 9 (2019), https://doi.org/10.3389/fpls.2018.01915.
Z. Qin, Y.-N. Wu, S. Li, Y. Zhang, Signaling between sporophytic integuments and developing female gametophyte during ovule development, Plant Sci. 335 (2023) 111829, https://doi.org/10.1016/j.plantsci.2023.111829.
L. Reiser, R.L. Fischer, The ovule and the embryo sac, Plant Cell (1993) 1291–1301, https://doi.org/10.1105/tpc.5.10.1291.
C.A. Schneider, W.S. Rasband, K.W. Eliceiri, NIH Image to ImageJ: 25 years of image analysis, Nat. Methods (2012), https://doi.org/10.1038/nmeth.2089.
K. Schneitz, M. Hülskamp, S.D. Kopczak, R.E. Pruitt, Dissection of sexual organ ontogenesis: a genetic analysis of ovule development in *Arabidopsis thaliana*, Development 124 (1997) 1367–1376, https://doi.org/10.1242/dev.124.7.1367.
K. Schneitz, M. Hülskamp, R.E. Pruitt, Wild-type ovule development in *Arabidopsis thaliana*: a light microscope study of cleared whole-mount tissue, Plant J. 7 (1995) 731–749, https://doi.org/10.1046/j.1365-313X.1995.07050731.x.
G.J. Seifert, K. Roberts, The biology of arabinogalactan proteins, Annu Rev. Plant Biol. 58 (2007) 137–161, https://doi.org/10.1146/annurev.arplant.58.032806.103801.
A.M. Showalter, Arabinogalactan-proteins: structure, expression and function, Cell. Mol. Life Sci. (2001), https://doi.org/10.1007/PL00000784.
A.M. Showalter, D. Basu, Extensin and arabinogalactan-protein biosynthesis: glycosyltransferases, research challenges, and biosensors, Front Plant Sci. (2016), https://doi.org/10.3389/fpls.2016.00814.
J. Silva, R. Ferraz, P. Dupree, A.M. Showalter, S. Coimbra, Three Decades of Advances in Arabinogalactan-Protein Biosynthesis, Front Plant Sci. (2020), https://doi.org/10.3389/fpls.2020.610377.
M. Smallwood, E.A. Yates, W.G.T. Willats, H. Martin, J.P. Knox, Immunochemical comparison of membrane-associated and secreted arabinogalactan-proteins in rice and carrot, Planta 198 (1996), https://doi.org/10.1007/BF00620063.
D.R. Smyth, J.L. Bowman, E.M. Meyerowitz, Early flower development in Arabidopsis, Plant Cell 2 (1990), https://doi.org/10.1105/tpc.2.8.755.
K. Sun, K. Hunt, B.A. Hauser, Ovule abortion in Arabidopsis triggered by stress, Plant Physiol. 135 (2004), https://doi.org/10.1104/pp.104.043091.
H. Tan, W. Liang, J. Hu, D. Zhang, MTR1 encodes a secretory fasciclin glycoprotein required for male reproductive development in rice, Dev. Cell 22 (2012), https://doi.org/10.1016/j.devcel.2012.04.011.
M.R. Tucker, A.M.G. Koltunow, Traffic monitors at the cell periphery: The role of cell walls during early female reproductive cell differentiation in plants, Curr. Opin. Plant Biol. (2014), https://doi.org/10.1016/j.pbi.2013.11.015.
M.R. Tucker, T. Okada, Y. Hu, A. Scholefield, J.M. Taylor, A.M.G. Koltunow, Somatic small RNA pathways promote the mitotic events of megagametogenesis during female reproductive development in Arabidopsis, Development 139 (2012), https://doi.org/10.1242/dev.075390.
A.J. Van Hengel, A. Van Kammen, S.C. De Vries, A relationship between seed development, Arabinogalactan-proteins (AGPs) and the AGP mediated promotion of somatic embryogenesis, Physiol. Plant 114 (2002) 637–644, https://doi.org/10.1034/j.1399-3054.2002.1140418.x.
J.R. Wendrich, D. Weijers, The <scp>A</scp> rabidopsis embryo as a miniature morphogenesis model, N. Phytol. 199 (2013) 14–25, https://doi.org/10.1111/nph.12267.
S. Wolf, Cell wall signaling in plant development and defense, Annu Rev. Plant Biol. 73 (2022) 323–353, https://doi.org/10.1146/annurev-arplant-102820-095312.
R. Yadegari, Female gametophyte development, Plant Cell Online 16 (2004) S133–S141, https://doi.org/10.1105/tpc.018192.
Y. Zhang, M.A. Held, D. Kaur, A.M. Showalter, CRISPR-Cas9 multiplex genome editing of the hydroxyproline-O-galactosyltransferase gene family alters arabinogalactan-protein glycosylation and function in Arabidopsis, BMC Plant Biol. 21 (2021) 16, https://doi.org/10.1186/s12870-020-02791-9.
Y. Zhang, M.A. Held, A.M. Showalter, Elucidating the roles of three β-glucuronosyltransferases (GLCATs) acting on arabinogalactan-proteins using a CRISPR-Cas9 multiplexing approach in Arabidopsis, BMC Plant Biol. 20 (2020), https://doi.org/10.1186/s12870-020-02420-5.
J. Zhong, Y. Ren, M. Yu, T. Ma, X. Zhang, J. Zhao, Roles of arabinogalactan proteins in cotyledon formation and cell wall deposition during embryo development of Arabidopsis, Protoplasma 248 (2011) 551–563, https://doi.org/10.1007/s00709-010-0204-y.
H.C. Zhou, L. Jin, J. Li, X.J. Wang, Altered callose deposition during embryo sac formation of multi-pistil mutant (*mp1*) in *Medicago sativa*, Genet. Mol. Res. 15 (2016), https://doi.org/10.4238/gmr.15027968.
K. Zhou, Glycosylphosphatidylinositol-anchored proteins in arabidopsis and one of their common roles in signaling transduction, Front Plant Sci. 10 (2019), https://doi.org/10.3389/fpls.2019.01022.